Supporting Information

Pseudocapacitive Gels Based on Conjugated Polyelectrolytes: Thickness and Ion Diffusion Limitations

Ricardo Javier Vázquez[a,b,+], Glenn Quek[b,+], Yan Jiang[b], Benjamin Yi Rui Peng[b], Samantha R. McCuskey[b,c], David Ohayon[b], Binu Kundukad[c], Xuehang Wang[d], and Guillermo C. Bazan[a,b,c,*]

Dr. R.J. Vázquez and Prof. G.C. Bazan

[a] Institute for Functional Intelligent Materials, National University of Singapore, Singapore 117544

Dr. R.J. Vázquez, G. Quek, Y. Jiang, Dr. S.R. McCuskey, Dr. D. Ohayon, B.Y.R. Peng, Prof. G.C. Bazan

[b] Departments of Chemistry and Chemical & Biomolecular Engineering, National University of Singapore, Singapore 119077, Singapore

Dr. S. R. McCuskey, Dr. B. Kundakad, and Prof. G.C. Bazan

[c] Singapore Centre for Environmental Life Sciences Engineering, Nanyang Technological University, Singapore 639798, Singapore

Prof. X. Wang

[d] Department of Radiation Science and Technology, Delft University of Technology, Delft 2629 JB, The Netherlands

[*] **Corresponding Author**: chmbgc@nus.edu.sg

[+] These authors contributed equally.

1. Materials and Methods

1.1 Materials: All chemicals used in this study were purchased from Fisher Scientific or Sigma Aldrich and used as received unless otherwise indicated. CPE-K was synthesized and characterized according to previous protocols.[1]. ^{1}H NMR (500 MHz, DMSO-d6) δ 8.48 – 7.95 (m, 4H), 3.25 – 2.97 (m, 16H), 2.43 2.13 (m, 4H), 2.06 – 1.79 (m, 4H), 1.55 (p, 20H), 1.29 (q, 16H), 1.20 – 0.95 (m, 4H), 0.89 (t, 24H). GPC (DMF) *Mn* = 31, 959 Da, *Mw* = 78, 852 Da, PDI = 2.47

1.2 Rheological measurements: Rheological measurements were performed using Haake Mars 60 (Thermo Scientific) with a plate-cone geometry. The plate diameter and the cone angle were 35mm and 0.5^o, respectively, and the gap separation was 0.052 mm. Experiments were performed in a strain-controlled mode at a temperature of 23^{o}C. 100 µL of CPE-K was deposited onto the plate, and a frequency sweep was done at a constant strain of 0.01%. Rheology is a technique to understand viscoelastic solids' mechanical properties, i.e., materials that exhibit solid (elastic) and liquid (viscous) behavior.[2] Therefore, the rheology technique offers further opportunities to understand the micro-domains that encompass the differences in physical properties of the gel depending on the electrolyte selection. In principle, rheology allows measuring the system response to applied forces at different rates (frequencies), creating a dynamical frequency sweep plot. An elastic (G') material will deform when subjected to an applied force and return to its original form when removed, implying a time-dependent substrate reorganization. Contrarily, in a viscous liquid (G''), a permanent deformation remains caused by irreversible slippage between substrate components. The difference in magnitude between the elastic modulus response (G') and the viscous modulus response (G'') will reveal the physical nature of the substrate.

The gels were measured after ion exchange following a similar step from section **1.4** (described below). After 2-4 days of ion exchange with the reservoir, the gels were removed from the working electrode and rheological characterization was carried out.

1.3 Working electrode fabrication: The gold-coated electrode fabrication consisted of heavily doped (ρ = 0.001-0.005 Ω cm) p + (boron) silicon wafers obtained from Addison Engineering Inc. The metal electrode in the silicon well was defined by soft lithography (PDMS mask), anisotropic plasma etching (Plasma-Therm DSEIII), and subsequent electron-beam evaporation of Ti (5 nm) and Au (70 nm). The depth of the Si well (247 ± 5 µm) was characterized by profilometry and SEM cross-sections. For electrode fabrication, ohmic contact to the device chip was made by rubbing Ga-In eutectic on its posterior. Then the chip was fixed to Ti-foil with carbon tape, providing a point of contact for electrical leads. Non-conductive silicon rubber gasket with a defined well was purchased from FuellCellStore (590363) and used as the spacers for creating the ~ 500 µm thick, 750 µm thick, and 1,250 µm thick working electrodes, see ***Figure S1***.[3,4]

1.4 Working electrode well loading: The CPE-K solid was first weighted, then diluted and vortexed with Milli-Q water to achieve a 20 mg/mL concentration. 100 µL, 200 µL, 300 µL, and or 1,250 µL of the prepared hydrogel was transferred into the working electrode well via pipette to lead gels with 250 µm, 500 µm, 750 µm, and 1,250 µm thickness, respectively. To precisely control the assembly process, working electrodes were adhered to the electrochemical cell's bottom lid, placed in an -80 ˚C freezer for 2-3 minutes, and then quickly sandwiched with the dialysis membrane, sealing O-ring, and 3-electrode chamber. It is important to note that the dialysis membrane confines the CPE-K hydrogel in the working electrode well.

1.5 Three-electrode electrochemical cells (3ECs): Single-chamber 3ECs were fabricated from acrylic to yield a 15 mL working volume and sealed with silicone O rings. An Ag/AgCl (3 M saturated KCl) reference electrode with a 6 mm diameter from LATECH was used. A 1.5 cm x 1 cm x 0.5 cm carbon-felt sewn with 0.25 mm Ti wire (Aldrich) was used as the counter electrode. A regenerated cellulose dialysis membrane with a 3.5 kD molecular weight cut-off (Repligen/Spectrum Laboratories) was used to confine the CPE-K hydrogel within the electrode well. The supporting electrolyte solutions were added posterior to the hydrogel, which was confined in the working electrode well. The temperature was kept at 25 .° C

1.6 Supporting electrolyte solution used in the 3ECs for experimentation. 2 M NaCl, 2 M $MgCl_2$, and 2 M $MgSO_4$.

1.7 Cyclic voltammetry (CV): Electrochemical characterization with CV was undertaken every 24 h from the start of experimentation to characterize the self-assembling properties of the hydrogel. For these experiments, the working electrode potential was swept from $E_{initial}$ = - 0.5 V to E_{vertex} = 0.6 V and back to E_{final} = - 0.6 V at different scan rates. This potential window prevented solvent breakdown and gold-working electrode oxidation. CVs were performed using a Biologic potentiostat (VMP300).

1.8 Chronoamperometry (CA): Using a Biologic potentiostat (VMP300), the hydrogels were poised at E_{CA} = 0.3 V vs. Ag/AgCl between every CV and EIS measurement. CA was performed using a Biologic potentiostat (VMP300).

1.9 Galvanostatic Charge-Discharge (GCD): The composites were subjected to GCD measurements after the conducting network was formed using a Biologic potentiostat (VMP300). GCD measurements were performed with a charge/discharge current Density of 0.5 mA (0.25 A g^{-1}) to 20 mA (10 A g^{-1}). Cycling stability was measured at 1 A g^{-1}. The specific charge/discharge current is calculated based on the mass of the composite. The potential window in GCD measurements (0.2–0.6 V vs. Ag/AgCl) is selected based on the redox potentials of CPE-K and Au oxidation.

1.10 Theoretical capacitance (C_{Th}) calculation for conjugated polymers: The theoretical capacitance of a conjugated polymer could be estimated by the following ***Equation S1***:

$$C_{Th} = \frac{\alpha * F}{\Delta E * M} \qquad \textbf{\textit{Equation S1}}$$

where α is the doping level per monomer unit, F is the Faraday constant (C mol^{-1}), ΔE is the operating voltage range (V), and M is the molecular weight of the monomer (g mol^{-1}). Based on this equation, the C_{Th} for the investigated CPE-Ks provides an estimate of α.[5]

1.11 Electrochemical impedance spectroscopy (EIS): Electrochemical characterization with EIS was measured every 24 h since the start of experimentation to characterize the self-assembling properties of the hydrogel. For these experiments, the working electrode potential was poised at E_{DC} = 0.3 V vs. Ag/AgCl, and a sinusoidal potential with amplitude E_{AC} = ±10 mV vs. Ag/AgCl was applied to start from a frequency of 100 kHz to 100 mHz. The EIS spectra fits the simplest appropriate equivalent circuit models using Bio-logic EC-Lab software to estimate charge transfer resistance, R_{CT}. The intersection of the Nyquist

curve at the Z_{Real} axis in the high-frequency range represents the solution resistance (R_E). The semicircle at high frequency can be modeled with a parallel combination of a constant phase element (Q_{geom}) and charge transfer resistance (R_{CT}). To fit spectra with a ~ 45˚ linear response at low frequencies, a circuit element called Warburg impedance, *W*, is added in series. This approach gives the simplest equivalent circuit $R_E + (Q_{geom}/R_{CT}) + W$. For EIS data with a more vertical linear response at low frequencies, an interfacial capacitance (Q_{int}) is used in place of the Warburg element, giving the equivalent circuit $R_E + (Q_{geom}/R_{CT}) + Q_{int}$. In all cases, a constant phase element "Q" is used in place of a pure capacitor element to represent the deviation from an ideal capacitor.

The Warburg resistance contributions can be obtained by analyzing the response of Z' versus the inverse of the square root of the angular frequency ($\omega^{-1/2}$), as shown in **Equation S2**:

$$Z' = R_E + R_{CT} + \sigma\omega^{-1/2} \qquad \textbf{Equation S2}$$

where R_E is the resistance between the electrolyte and the electrode, R_{CT} is the charge transfer resistance, ω is the angular frequency, and σ is the Warburg factor.[6] Based on this relationship, the slope of the linearly fitted lines of Z' vs. $\omega^{-1/2}$ provides σ.

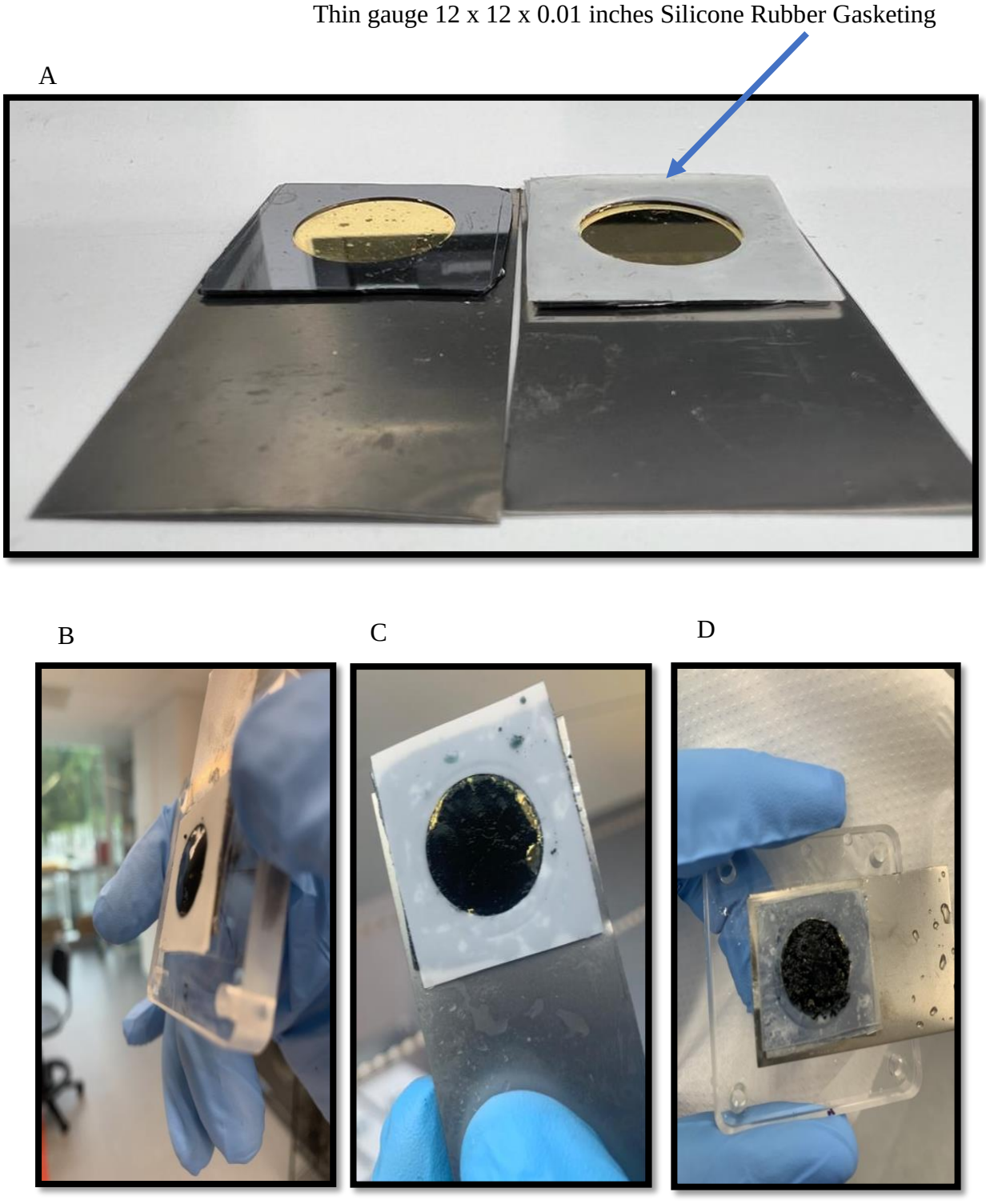

Figure S1. Representative ~ 250 μm (left) and 500 μm (right) thick working electrodes (**A**). Representative thick gel before (**B**), after (**C**) ion exchange, and (**D**) after ion exchange and electrochemical characterization.

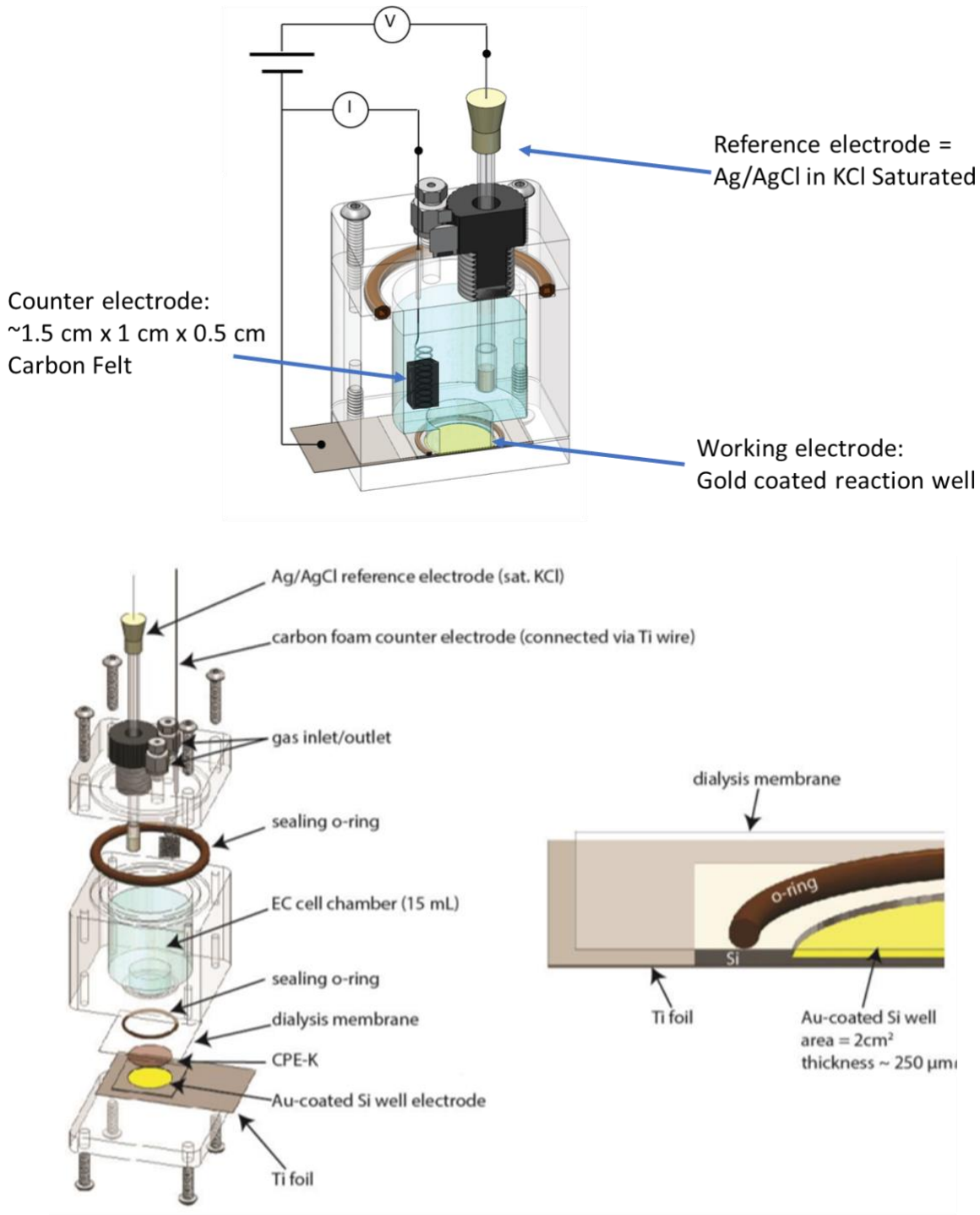

Figure S2. Schematics of the 3-electrodes electrochemical cell used in this study, as similarly reported in previous studies.[1,3] The working electrode is realized by drop-casting and confining 100 μL of the CPE-K hydrogel inside a gold-coated well (area ≈ 2 cm^2, depth ≈ 250 μm). A dialysis membrane (3.5 kD MWCO) was employed to restrict the hydrogel within the electrode and promote ion exchange. Similar diagram could be found in r

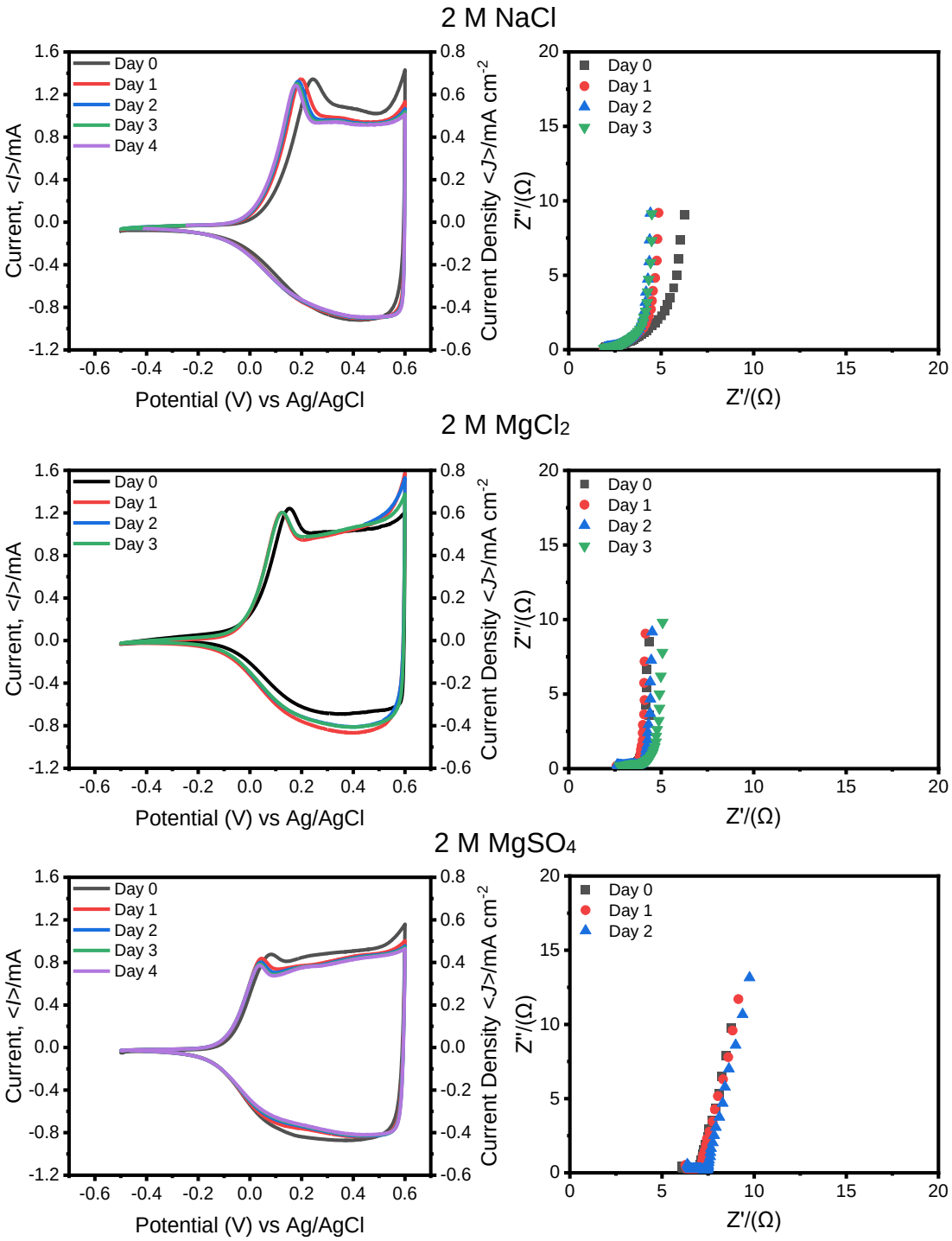

Figure S3. CV and EIS progression by day of the CPE-K gels with 250 µm thickness in different electrolytes. Scan rate is 5 mV s^{-1}. In all cases, scans started from negative potentials.

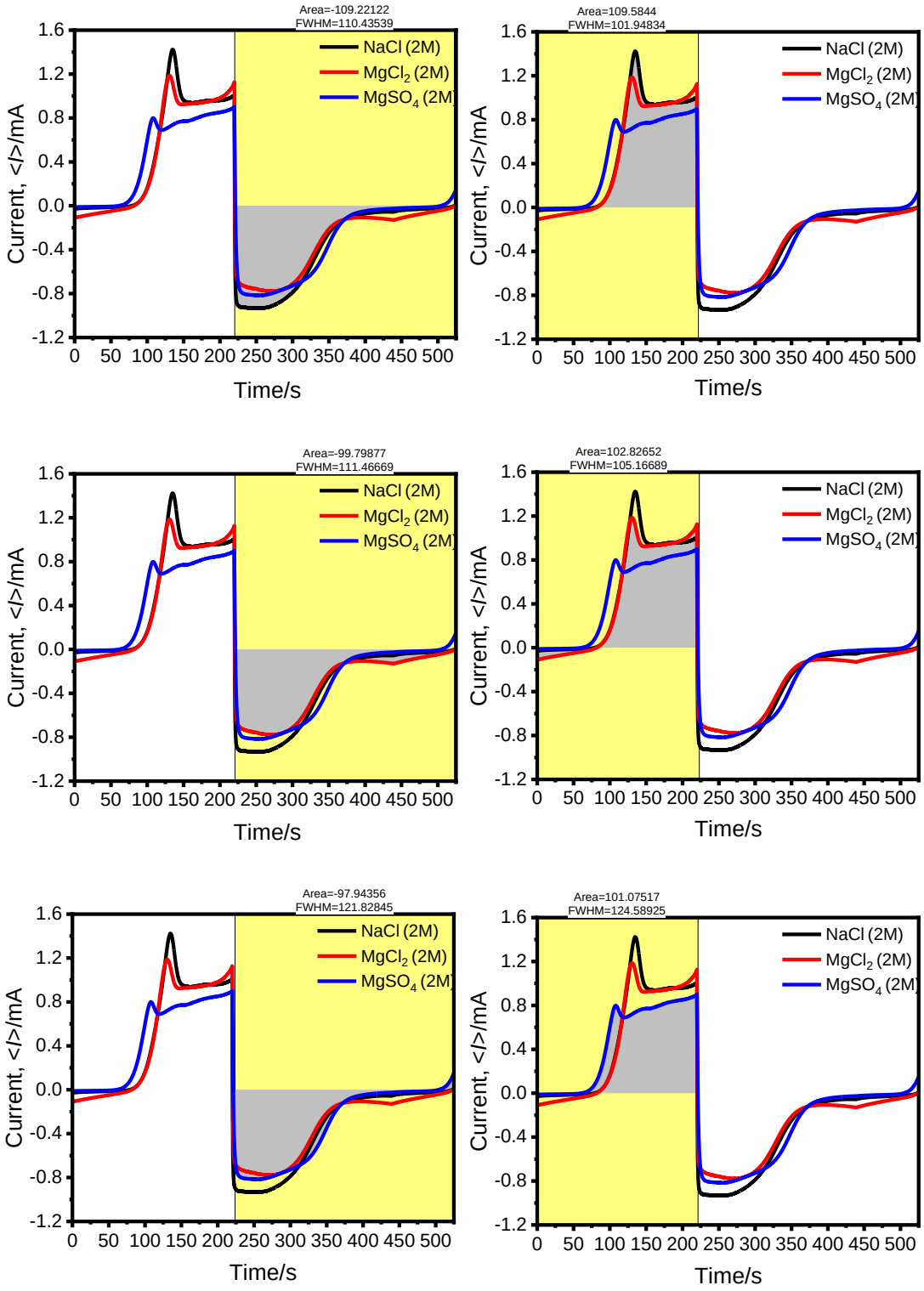

Figure S4. Current response (< *I* >) in function of time for the thinner CPE-K gels in different electrolyte solutions at 5 mV s^{-1}. This measurement allows the determination of the systems' Coulombic efficiency (Q) in different conditions by dividing the discharge area over the charging area.

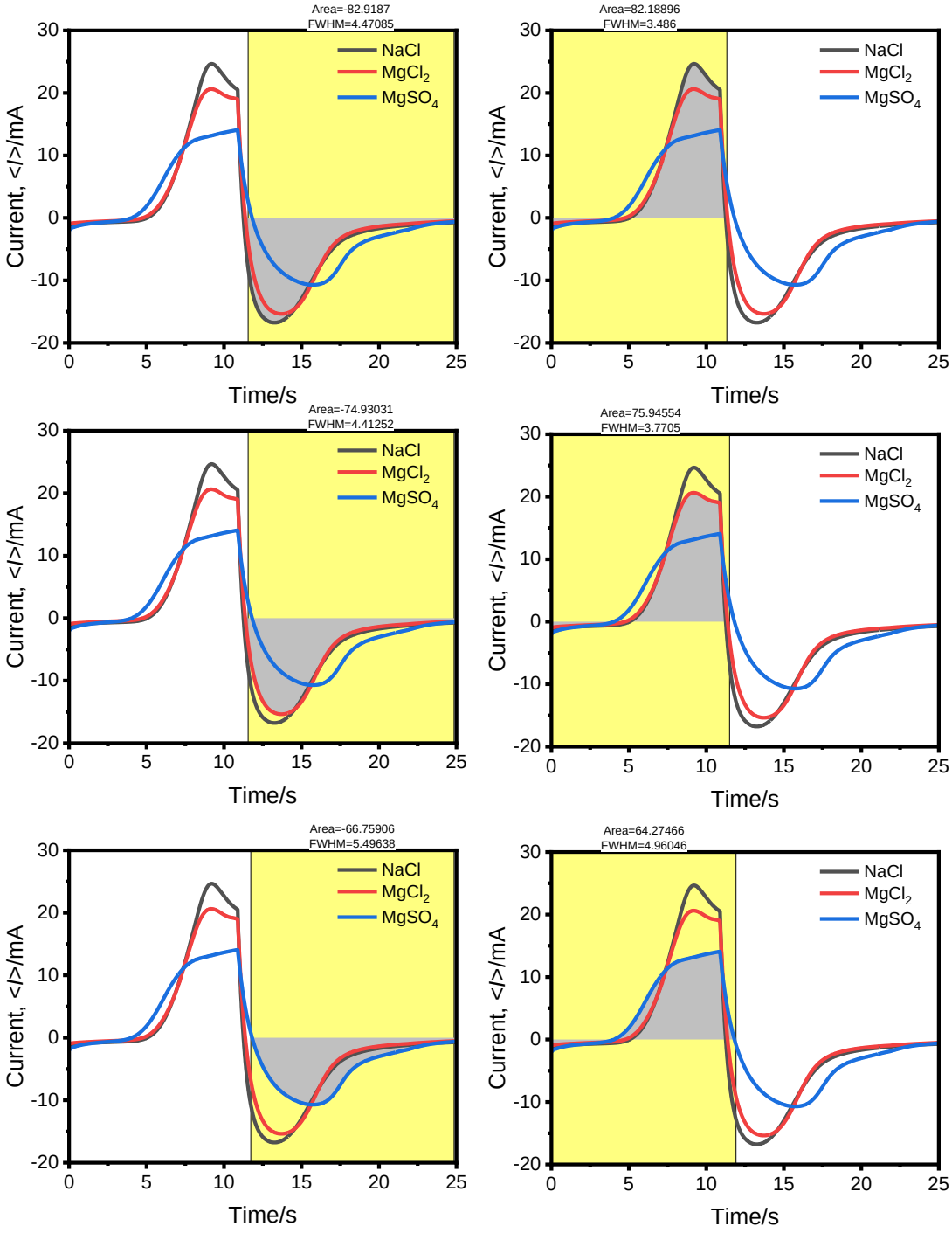

Figure S5. Current response (< *I* >) in function of time for the thinner CPE-K gels in different electrolyte solutions at 100 mV s^{-1}. This measurement allows the determination of the systems' Coulombic efficiency (Q) in different conditions by dividing the discharge area over the charging area.

Table S1. The C_{Areal} (mF cm^{-2}) capacitance of 20 mg/mL CPE-K in different electrolytes at specific currents.

Material	C_{Areal} (mF cm^{-2})	Current Density (mA cm^{-2})
CPE-K (2M NaCl; This Work)	92 ± 4	0.25
	90 ± 3	0.5
	89 ± 3	0.75
	88 ± 4	1
	82 ± 3	2.5
	76 ± 4	5
	70 ± 4	7.5
	65 ± 4	10
	56 ± 4	15
	45 ± 5	20
	32 ± 6	25
	19 ± 4	30
CPE-K (2M $MgCl_2$; This Work)	81 ± 4	0.25
	78 ± 3	0.5
	77 ± 4	0.75
	76 ± 3	1
	75 ± 4	2.5
	71 ± 3	5
	67 ± 8	7.5
	61 ± 3	10
	53 ± 5	15
	39 ± 5	20
	20 ± 11	25
	10 ± 9	30
CPE-K (2M $MgSO_4$; This Work)	82 ± 2	0.25
	80 ± 2	0.5
	76 ± 2	0.75
	72 ± 3	1
	62 ± 6	2.5
	50 ± 5	5
	40 ± 3	7.5
	24 ± 5	10
	1 ± 0	15
	1 ± 0	20
	1 ± 0	25
	1 ± 0	30
CPE-K (SBS + Mg^{2+})[1]	88 ± 4	0.25
	85 ± 2	0.5
	82 ± 2	0.75
	80 ± 2	1
	70 ± 5	2.5
CPE-K + (SBS + Mg^{2+})[4]	80	0.25
CPE-K + (2D Electrolyte; Graphene) [4]	80	0.25
CPE-K + (Mg^{2+})[7]	70	0.25

Table S2. The **specific capacitance** of 20 mg/mL of CPE-K in different electrolytes at specific currents and their respective doping percentage (α).

Specific Current ($A\ g^{-1}$)	Specific Capacitance ($F\ g^{-1}$)			α		
($A\ g^{-1}$)	2 M NaCl	2 M MgCl2	2 M MgSO4	2 M NaCl	2 M MgCl2	2 M MgSO4
0.25	92.00	81.00	82.00	0.26	0.22	0.23
0.5	90.00	78.00	80.00	0.25	0.22	0.22
0.75	89.00	77.00	76.00	0.25	0.21	0.21
1	88.00	76.00	72.00	0.24	0.21	0.20
2.5	82.00	75.00	62.00	0.23	0.21	0.17
5	76.00	71.00	50.00	0.21	0.20	0.14
7.5	70.00	67.00	40.00	0.19	0.19	0.11
10	65.00	61.00	24.00	0.18	0.17	0.07
15	56.00	53.00	1.00	0.16	0.15	0.00
20	45.00	39.00	1.00	0.12	0.11	0.00
25	32.00	20.00	1.00	0.09	0.06	0.00
30	19.00	10.00	1.00	0.05	0.03	0.00

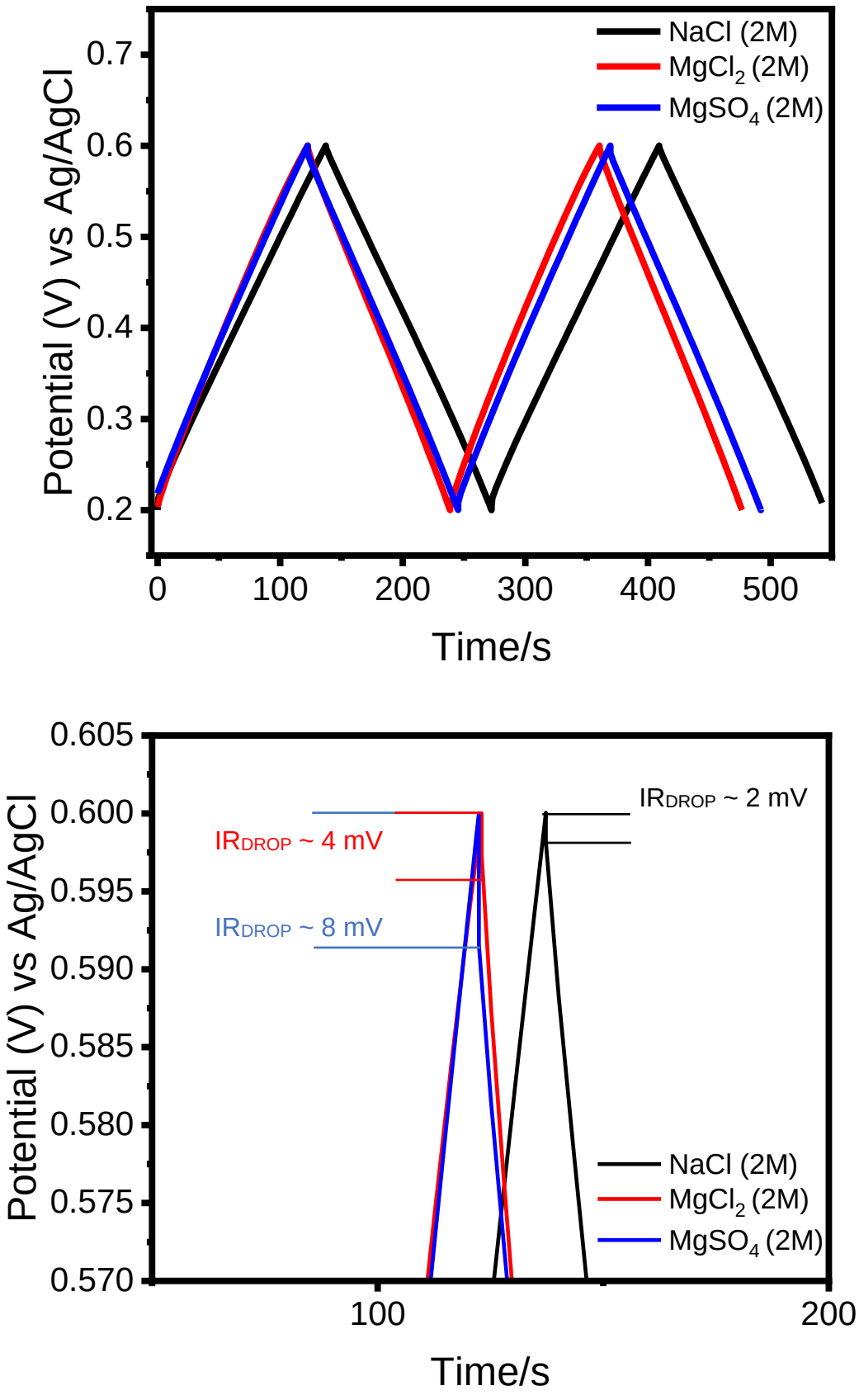

Figure S6. Representative charge/discharge curves of the investigated CPE-K hydrogels in different electrolyte solutions for the determination of voltage loss (IR_{DROP}).The bottom figure is a close up from the top figure to appreciate the IR drops.

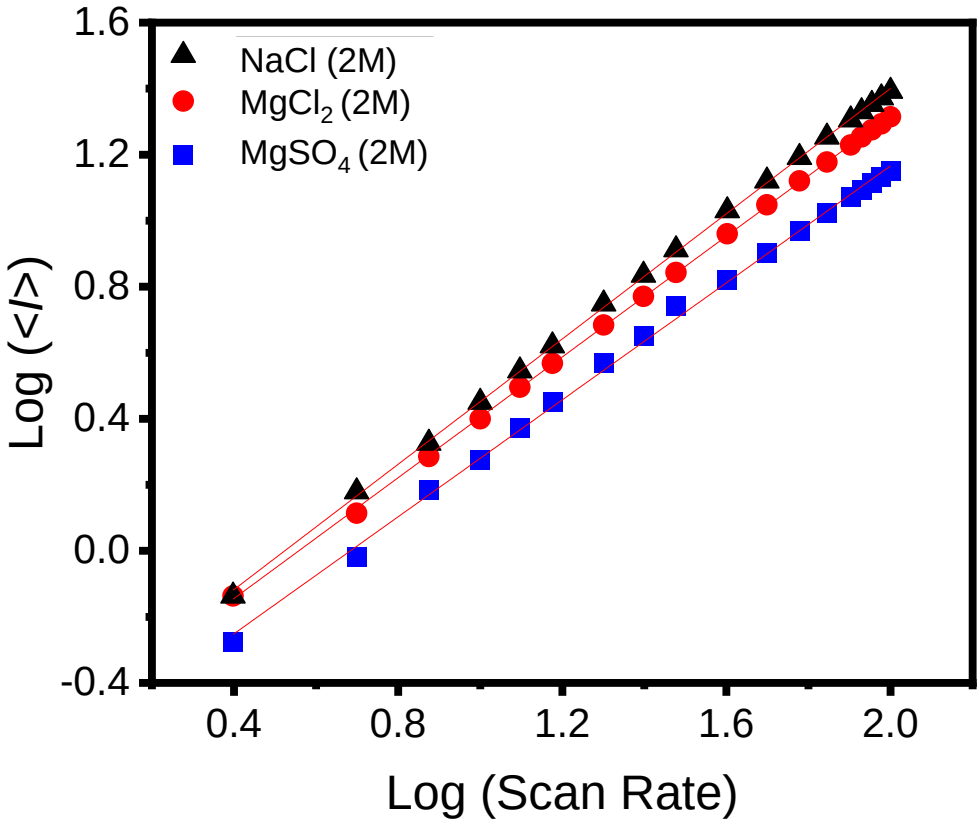

2M NaCl

Equation	y = a + b*x
Plot	H
Weight	No Weighting
Intercept	-0.49673 ± 0.005
Slope	0.94874 ± 0.0038
Residual Sum of Squa	9.7666E-4
Pearson's r	0.99987
R-Square (COD)	0.99973
Adj. R-Square	0.99972

2M $MgCl_2$

Equation	y = a + b*x
Plot	G
Weight	No Weighting
Intercept	-0.51013 ± 0.00439
Slope	0.91456 ± 0.00287
Residual Sum of Squares	5.35057E-4
Pearson's r	0.99992
R-Square (COD)	0.99984
Adj. R-Square	0.99983

2M $MgSO_4$

Equation	y = a + b*x
Plot	F
Weight	No Weighting
Intercept	-0.60543 ± 0.013
Slope	0.88575 ± 0.0091
Residual Sum of Squa	0.00536
Pearson's r	0.99916
R-Square (COD)	0.99831
Adj. R-Square	0.99821

Figure S7. Log-Log plot of current < *I* > vs. scan rate for the 250 µm thick hydrogels in different electrolytes.

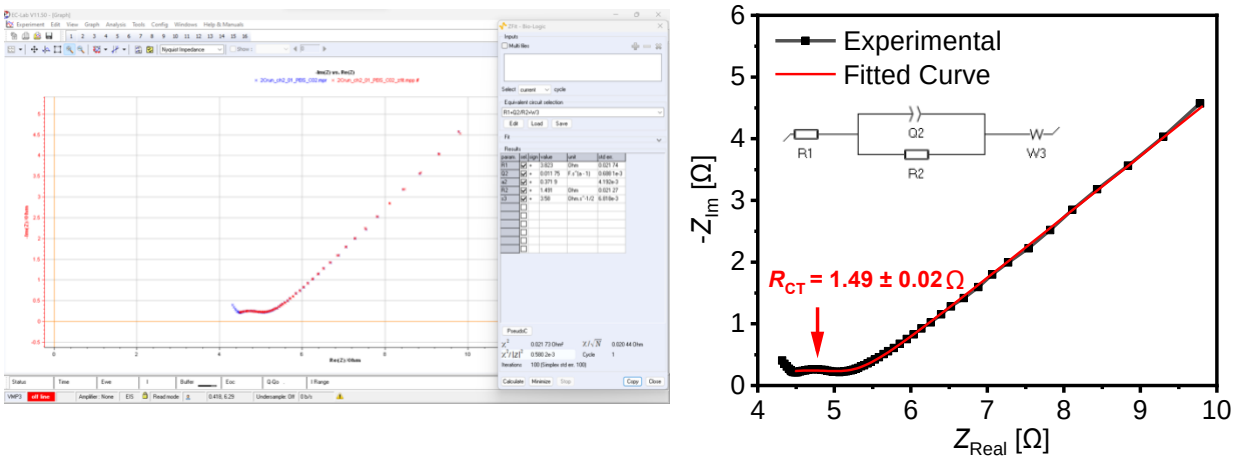

Figure S8. Representative EIS Fitted curve for the CPE-K gel in 2M NaCl electrolyte from the BioLogic EC-Lab software and its fitted curve using the equivalent circuit shown for the CPE-K gel in 2M NaCl electrolyte.

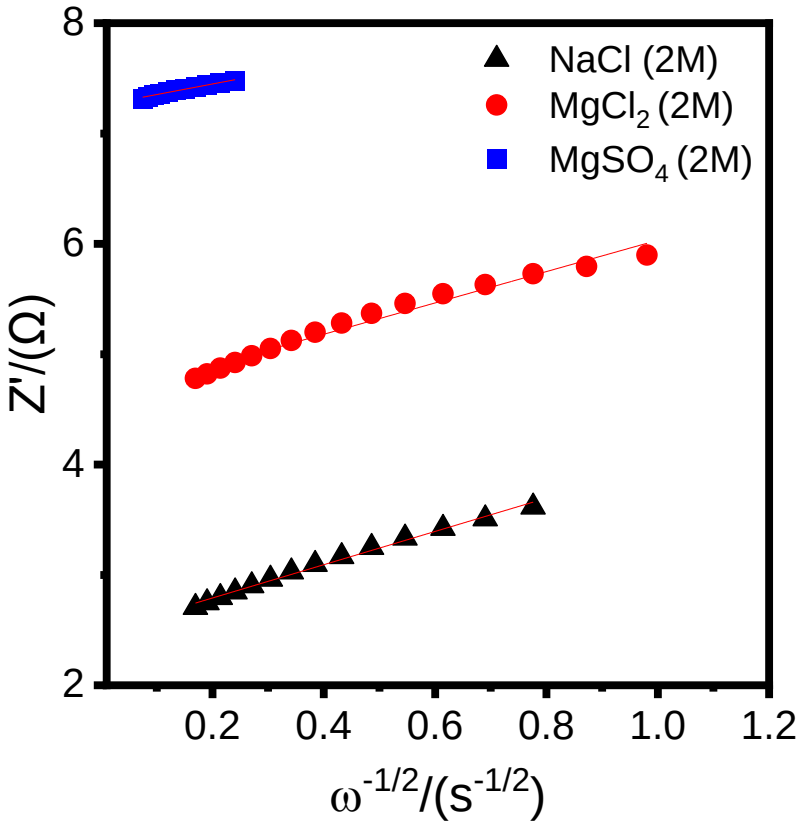

2M NaCl

Equation	y = a + b*x
Plot	P
Weight	No Weighting
Intercept	2.48917 ± 0.01
Slope	1.50813 ± 0.03
Residual Sum of Squ	0.00848
Pearson's r	0.9962
R-Square (COD)	0.99241
Adj. R-Square	0.99178

2M $MgCl_2$

Equation	y = a + b*x
Plot	O
Weight	No Weighting
Intercept	4.52728 ± 0.019
Slope	1.67817 ± 0.047
Residual Sum of Squa	0.00829
Pearson's r	0.99568
R-Square (COD)	0.99138
Adj. R-Square	0.9906

2M $MgSO_4$

Equation	y = a + b*x
Plot	Z'/(Ω)
Weight	No Weighting
Intercept	7.25749 ± 0.00
Slope	0.95584 ± 0.03
Residual Sum of Squa	4.148E-4
Pearson's r	0.99255
R-Square (COD)	0.98516
Adj. R-Square	0.98351

Figure S9. Warburg factor determination for the gels with d_{Thk} = 250 µm in different electrolytes.

Table S3. The C_{Areal} of 20 mg/mL CPE-K gels in 2 M NaCl with different thicknesses at different current densities < *J* >.

	C_{Areal} (mF cm^2)			
Current Density < *J* > (mA cm^{-2})	250 µm	500 µm	750 µm	1,250 µm
0.25	92 ± 4	194 ± 15	298 ± 11	523 ± 5
0.5	90 ± 3	191 ± 14	297 ± 12	515 ± 2
0.75	89 ± 3	187 ± 13	293± 13	491 ± 2
1	88 ± 4	182 ± 11	284 ± 8	482 ± 4
2.5	82 ± 3	160 ± 5	264 ± 13	432 ± 5
5	76 ± 4	136 ± 3	237 ± 12	352 ± 3
7.5	70 ± 4	118 ± 8	215 ± 12	283 ± 1
10	65 ± 4	103 ± 10	195 ± 10	205 ± 1
15	56 ± 4	70 ± 12	153 ± 6	62 ± 2
20	45 ± 5	38 ± 8	102 ± 5	4 ± 1
25	32 ± 6	17 ± 2	52 ± 13	2 ± 2
30	19 ± 4	10 ± 3	20 ± 10	2 ± 1

Table S4. **The specific capacitance** of 20 mg/mL of CPE-K in 2M NaCl at different thicknesses and their respective doping percentage (α).

A g^{-1}	250 µm	α	A g^{-1}	500 µm	α	A g^{-1}	750 µm	α	A g^{-1}	1,250 µm	α	mA cm^{-2}
0.25	92.00	0.26	0.13	97.25	0.27	0.08	99.33	0.28	0.05	104.61	0.29	0.25
0.5	90.00	0.25	0.25	95.73	0.26	0.17	99.00	0.27	0.10	103.12	0.29	0.5
0.75	89.00	0.25	0.38	93.52	0.25	0.25	97.75	0.27	0.15	98.26	0.27	0.75
1	88.00	0.24	0.50	91.26	0.22	0.33	94.79	0.26	0.20	96.57	0.27	1
2.5	82.00	0.23	1.25	80.12	0.19	0.83	87.42	0.24	0.50	86.49	0.24	2.5
5	76.00	0.21	2.50	68.34	0.16	1.67	79.08	0.22	1.00	70.49	0.20	5
7.5	70.00	0.19	3.75	59.00	0.14	2.50	71.83	0.20	1.50	56.61	0.16	7.5
10	65.00	0.18	5.00	51.29	0.10	3.33	65.08	0.18	2.00	41.02	0.11	10
15	56.00	0.16	7.50	34.87	0.07	5.00	51.25	0.14	3.00	12.54	0.03	15
20	45.00	0.12	10.00	23.71	0.04	6.67	34.17	0.09	4.00	0.87	0.00	20
25	32.00	0.09	12.50	15.00	0.02	8.33	17.25	0.05	5.00	0.39	0.00	25
30	19.00	0.05	15.00	5.50	0.00	10.00	6.67	0.02	6.00	0.30	0.00	30

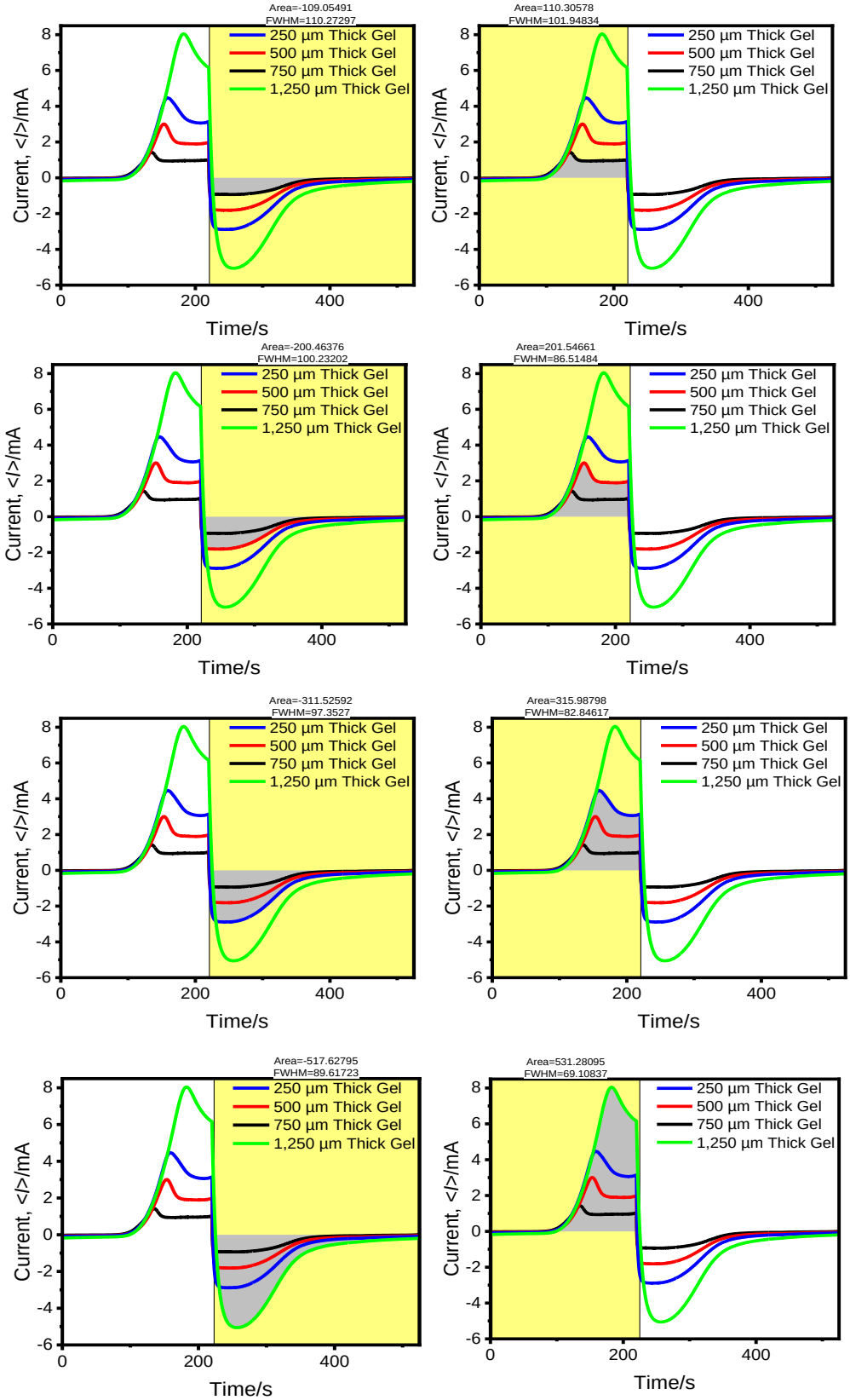

Figure S10. Current response in function of time for CPE-K hydrogels with different thickness. This measurement allows the determination of the systems' Coulombic efficiency (Q) in different conditions by dividing the discharge area over the charging area.

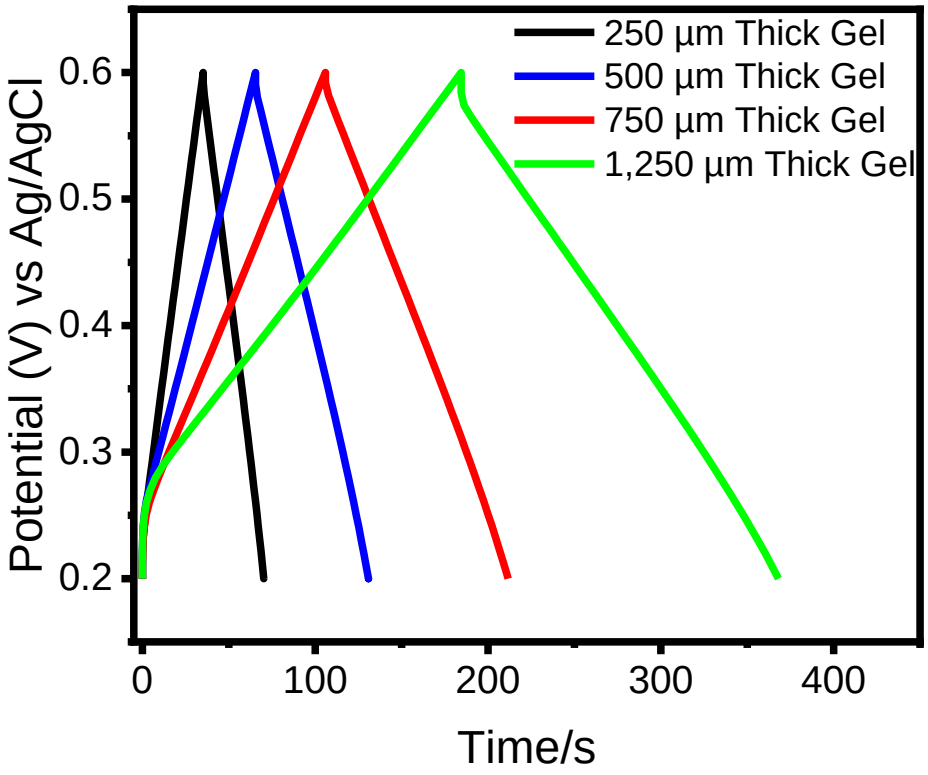

Figure S11. Representative charge/discharge curves of the investigated CPE-K hydrogels with different thicknesses at 1 mA cm^{-2} for determining voltage loss (IR_{DROP}). Electrolyte is NaCl (2 M).

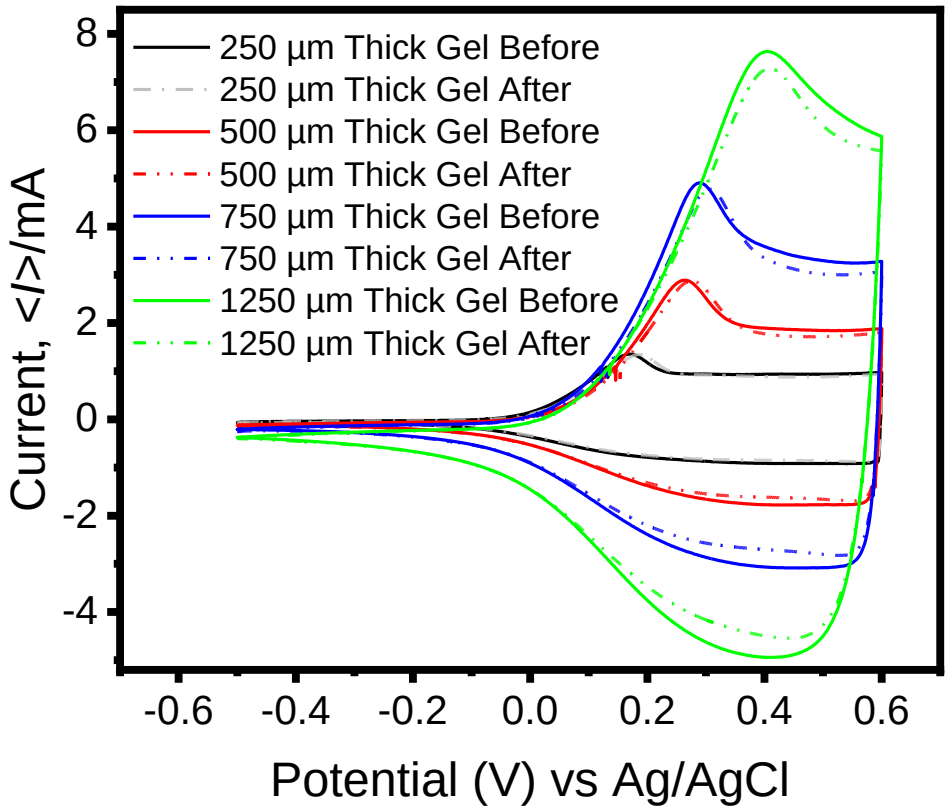

Figure S12. CV measurements of the CPE-K gels at different thickness before and after 100,000 charge discharge cycles.

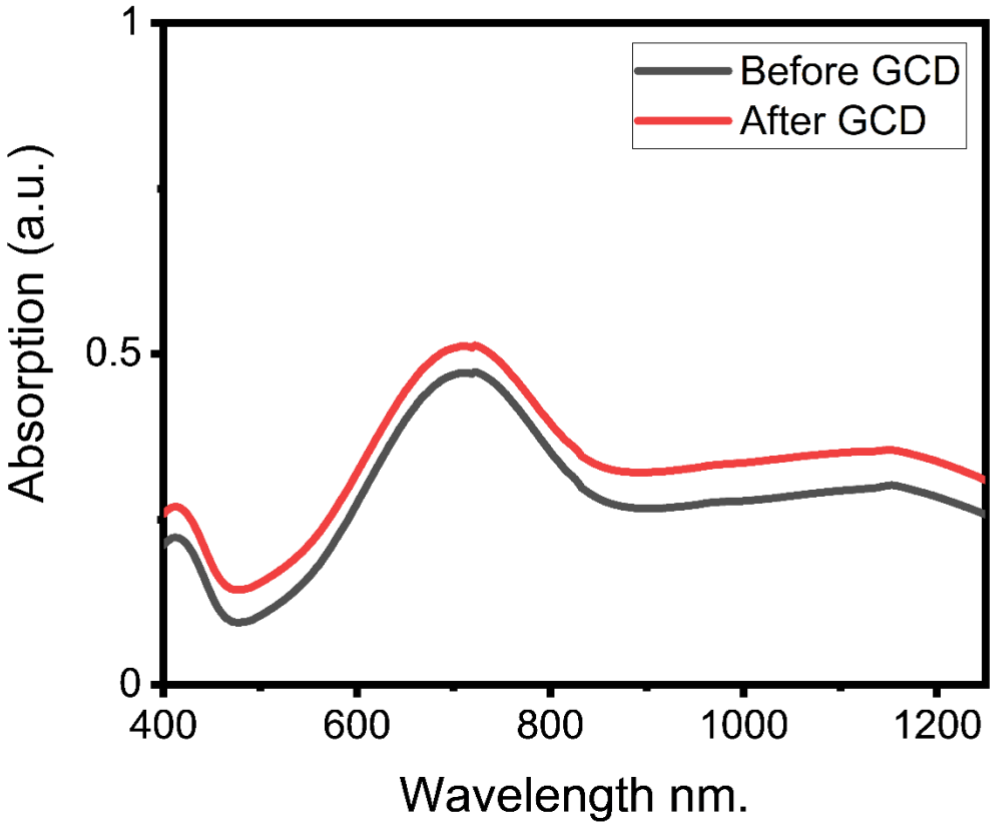

Figure S13. UV-VIS for CPE-K before and after GCD characterization.

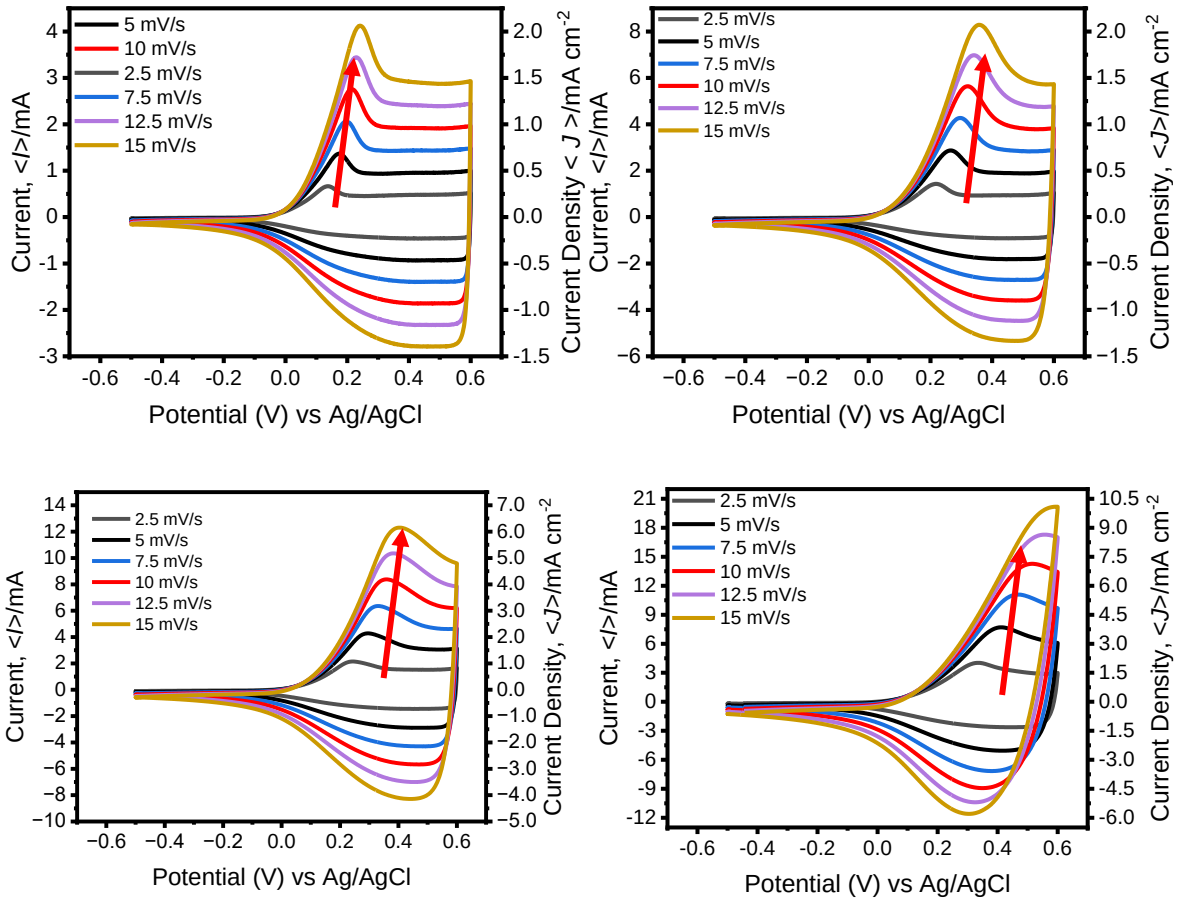

Figure S14. CV measurements for determining the areal capacitance of the CPE-K gels in Figure 6 and correlating the scan rates with the approximate current density used for low rates GCD measurements. In all cases, scans started from negative potentials.

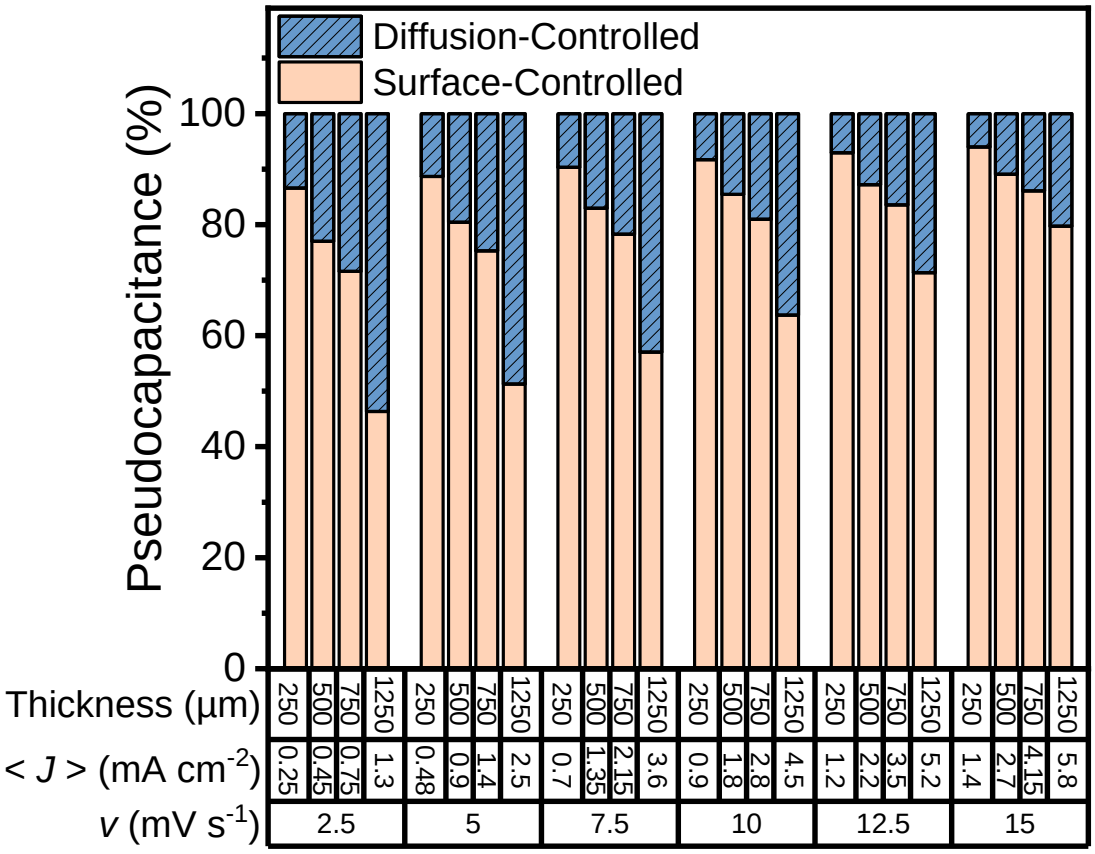

Figure S15. C_{Areal} percentage contributions from surface-controlled and diffusion-controlled processes at different rates.

Table S5. Summary of the data used for constructing information plotted for **Figure 5D.**

Scan rate(mV/s)	Thicness (µm)	Volume (µL)	CV-total	CV-pseudo	surface-controlled	diffusion-contolled	Areal Capacitance (mF/cm^2)	surface--controlled	diffusion-contolled
2.5	250	100	0.55	0.47	0.87	0.13	88.60	76.73	11.87
	500	200	1.01	0.77	0.77	0.23	171.00	131.68	39.32
	750	300	1.57	1.13	0.72	0.28	270.00	193.26	76.74
	1250	500	2.67	1.24	0.46	0.54	456.00	211.33	244.67
Scan rate(mV/s)	Thicness (µm)	Volume (µL)	CV-total	CV-pseudo	surface-controlled	diffusion-contolled	Areal Capacitance (mF/cm^2)	surface--controlled	diffusion-contolled
5	250	100	1.07	0.94	0.89	0.11	89.18	79.07	10.11
	500	200	1.93	1.55	0.80	0.20	166.82	134.16	32.66
	750	300	2.99	2.25	0.75	0.25	261.07	196.58	64.49
	1250	500	4.83	2.48	0.51	0.49	409.15	209.85	199.30
Scan rate(mV/s)	Thicness (µm)	Volume (µL)	CV-total	CV-pseudo	surface-controlled	diffusion-contolled	Areal Capacitance (mF/cm^2)	surface--controlled	diffusion-contolled
7.5	250	100	1.57	1.42	0.90	0.10	89.31	80.67	8.63
	500	200	2.80	2.32	0.83	0.17	163.07	135.28	27.79
	750	300	4.32	3.38	0.78	0.22	251.77	197.12	54.65
	1250	500	6.52	3.72	0.57	0.43	360.55	205.72	154.83
Scan rate(mV/s)	Thicness (µm)	Volume (µL)	CV-total	CV-pseudo	surface-controlled	diffusion-contolled	Areal Capacitance (mF/cm^2)	surface--controlled	diffusion-contolled
10	250	100	2.06	1.89	0.92	0.08	87.92	80.63	7.29
	500	200	3.63	3.10	0.85	0.15	159.48	136.27	23.21
	750	300	5.56	4.50	0.81	0.19	242.52	196.35	46.16
	1250	500	7.78	4.96	0.64	0.36	317.77	202.44	115.32
Scan rate(mV/s)	Thicness (µm)	Volume (µL)	CV-total	CV-pseudo	surface-controlled	diffusion-contolled	Areal Capacitance (mF/cm^2)	surface--controlled	diffusion-contolled
12.5	250	100	2.54	2.36	0.93	0.07	87.59	81.42	6.17
	500	200	4.44	3.87	0.87	0.13	155.71	135.78	19.93
	750	300	6.74	5.63	0.84	0.16	235.06	196.41	38.65
	1250	500	8.68	6.20	0.71	0.29	277.20	197.77	79.43
Scan rate(mV/s)	Thicness (µm)	Volume (µL)	CV-total	CV-pseudo	surface-controlled	diffusion-contolled	Areal Capacitance (mF/cm^2)	surface--controlled	diffusion-contolled
15	250	100	3.02	2.83	0.94	0.06	85.78	80.64	5.14
	500	200	5.22	4.65	0.89	0.11	152.80	136.11	16.69
	750	300	7.85	6.76	0.86	0.14	227.30	195.64	31.66
	1250	500	9.33	7.44	0.80	0.20	241.67	192.67	48.99

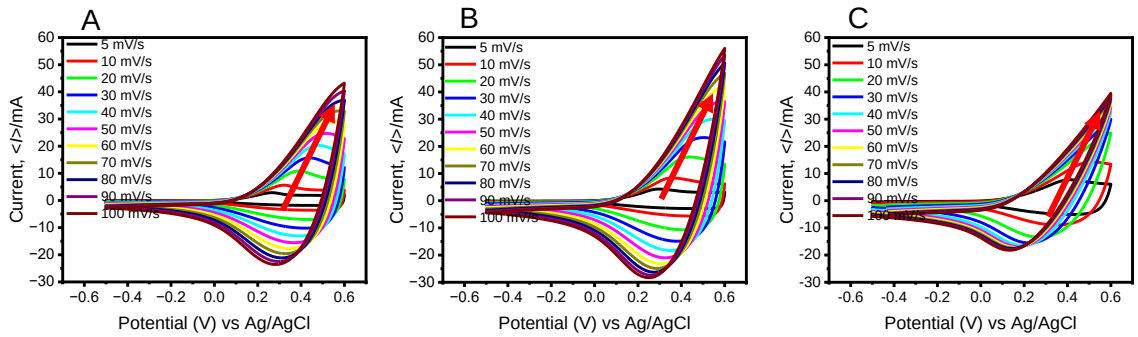

Figure S16. Scan-rate dependent CV traces of the investigated hydrogels in 2M NaCl at different thicknesses: (**A**) 500 µm, (**B**) 750 µm, and (**C**) 1,250 µm. In all cases, the scans started from the negative potential.

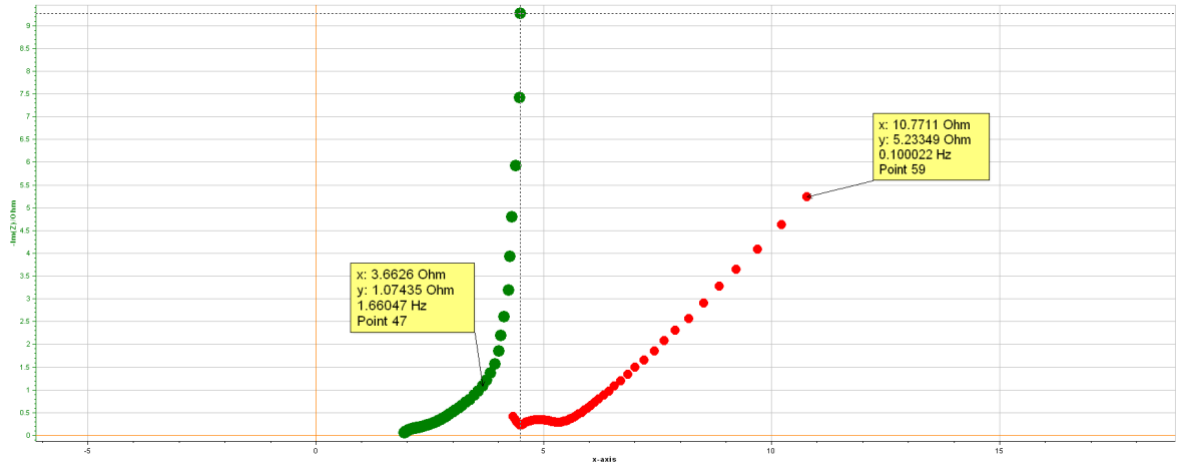

Figure S17. Nyquist plot for the 250µm d_{Thk} (Green) and 1,250µm d_{Thk} (Red) gels and the respective frequencies with Warburg Domains.

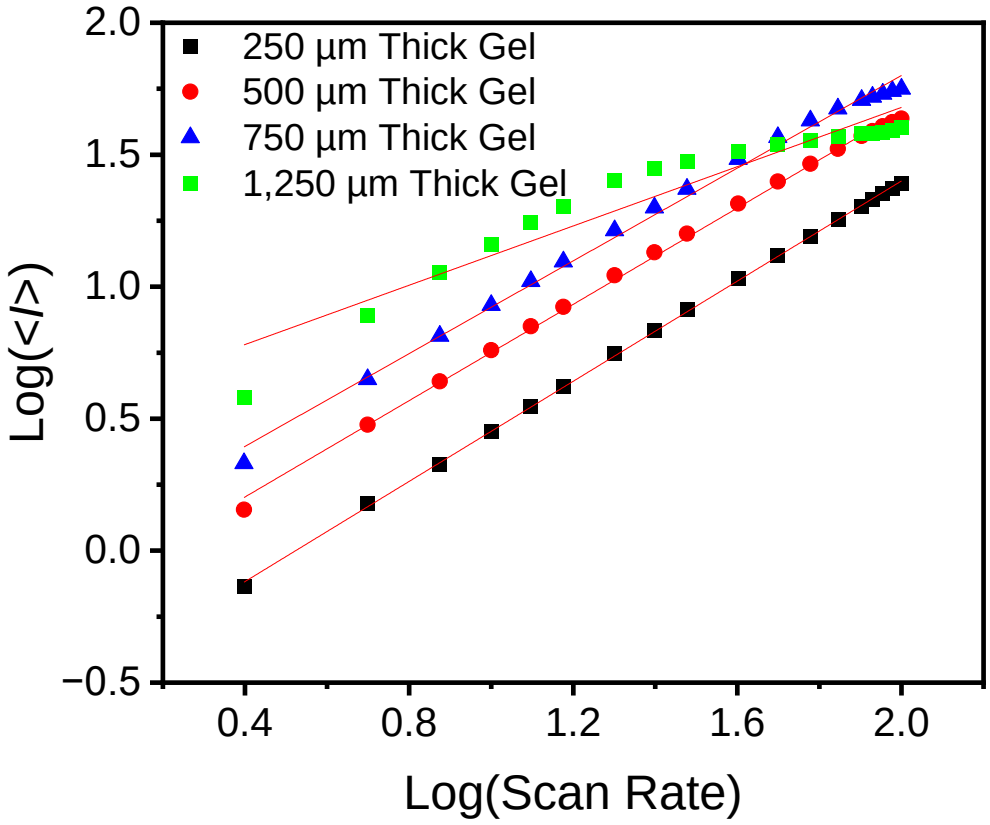

250 µm

Equation	y = a + b*x
Plot	F
Weight	No Weighting
Intercept	−0.49673 ± 0.0
Slope	0.94874 ± 0.00
Residual Sum of Sq	9.7666E−4
Pearson's r	0.99987
R-Square (COD)	0.99973
Adj. R-Square	0.99972

500 µm

Equation	y = a + b*x
Plot	G
Weight	No Weighting
Intercept	−0.16166 ± 0.013
Slope	0.9124 ± 0.0087
Residual Sum of Squa	0.00497
Pearson's r	0.99926
R-Square (COD)	0.99853
Adj. R-Square	0.99844

750 µm

Equation	y = a + b*x
Plot	H
Weight	No Weighting
Intercept	0.04361 ± 0.023
Slope	0.87852 ± 0.015
Residual Sum of Squ	0.0151
Pearson's r	0.99759
R-Square (COD)	0.99519
Adj. R-Square	0.99489

1,250 µm

Equation	y = a + b*x
Plot	yyy
Weight	No Weighting
Intercept	0.55621 ± 0.064
Slope	0.56163 ± 0.042
Residual Sum of Squar	0.11711
Pearson's r	0.95708
R-Square (COD)	0.916
Adj. R-Square	0.91075

Figure S18. Log-Log plot of current < *I* > vs. scan rate upon increasing the gel thickness.

References:

1 R. J. Vázquez, G. Quek, S. R. McCuskey, L. Llanes, B. Kundukad, X. Wang and G. C. Bazan, *J Mater Chem A Mater*, 2022, **10**, 21642–21649.

2 B. Kundukad, T. Seviour, Y. Liang, S. A. Rice, S. Kjelleberg and P. S. Doyle, *Soft Matter*, 2016, **12**, 5718–5726.

3 S. R. McCuskey, Y. Su, D. Leifert, A. S. Moreland and G. C. Bazan, *Advanced Materials*, 2020, **32**, 1908178.

4 Y. Su, S. R. McCuskey, D. Leifert, A. S. Moreland, L. Zhou, L. C. Llanes, R. J. Vazquez, L. Sepunaru and G. C. Bazan, *Adv Funct Mater*, 2021, **31**, 2007351.

5 K. D. Fong, T. Wang and S. K. Smoukov, *Sustain Energy Fuels*, 2017, **1**, 1857–1874.

6 W. Liu, H. Yi, Q. Zheng, X. Li and H. Zhang, *J Mater Chem A Mater*, 2017, **5**, 10928–10935.

7 R. J. Vázquez, S. R. McCuskey, G. Quek, Y. Su, L. Llanes, J. Hinks and G. C. Bazan, *Macromol Rapid Commun*, 2022, **43**, 2100840.